Developments in Environmental Science, Volume 5
D. Sarkar, R. Datta and R. Hannigan (Editors)

ISSN: 1474-8177/DOI:10.1016/S1474-8177(07)05030-9

Chapter 30

Characterizing the surface chemistry of oxides with X-ray photoelectron spectroscopy: Assessment regarding surface oxygen valence charge and acid–base properties

M. Ding and B.H.W.S. de Jong

For Titus

Abstract

Variations in valence charge of surficial O (Oxygen) atoms in a compound may be calculated from shifts in the O1s binding energies. Using the National Institute of Standards and Technology (NIST) photoelectron database, a consistent set of charges for O atoms in oxides can be made. It uses as reference frame a theoretical chemical procedure that incorporates a spherical potential around an O atom to account for the field generated by the surrounding atoms in a compound. The complete database indicates no strong correlations between calculated surface O charges and electronegativity, bulk or surface acid–base properties, points of zero charge or refractive index. To account for the large differences in surface acid–base properties, a detailed partitioning of charge on the O atom isolated from the surrounding atoms, a so-called atom in molecule assignment, rather than overall charge transfer must be invoked. It implies that the electron density associated with the O atomic orbitals in a molecular orbital must be partitioned between a bonded and a non-bonded part. The ratio between these two parts of the overall electron density varies, depending on the nature of the interaction between a specific metal atom and the O atoms in its coordination sphere. For silicates, this ratio is reasonably well established. Quantifying it from first principles for other metal–oxide moieties requires additional molecular orbital calculations.

30.1. Introduction

For many decades, structure, reactivity and properties of oxide materials have been studied in a variety of fields, including material science, inorganic chemistry, heterogeneous catalysis, glass and ceramic science, geochemistry, and environmental chemistry. In all these interdisciplinary research activities, much effort has been directed toward characterizing and predicting the surface reactivity of oxides, and in particular their acidic or basic character.

In aqueous solution, the acid–base concept is well defined and is fundamental to all chemistry. However, for solids it is not always obvious how acid–base concepts propagate in the different domains of chemistry. Thus in glass and ceramic science alkali and alkaline earth oxides are basic whereas silica is acidic. In heterogeneous catalysis, an acidic surface is defined as a proton-releasing surface as inferred from colorimetric titration with a basic indicator. In adsorption studies a surplus or deficit of surface protons is associated with a positive or negative surface charge. All these assignments suppose as basic ingredient a charge transfer from an electron source to an electron sink. It is the degree to which this transfer takes place that governs the adhesive and cohesive properties of a substance.

Donating or accepting electrons of elements that make up a substance have been at the root of all chemistry since the introduction of the concept of electronegativity by Berzelius in 1811. Though conceptually easy, it has been difficult to apply quantitatively to chemical processes. This manifests itself by the still in general insurmountable difficulties associated with the prediction of crystal structures from their chemical formulas only, as noted by Maddox (1988). Despite substantial efforts to remedy this, as he calls it, scandal in the physical sciences the issue is by no means settled yet. Sometimes the deficiency is obvious, for instance when using two rather than three body potentials in tetrahedral coordinated solids, more often it is not.

Though already difficult for solids for which accurate crystal structures are known, the problem is compounded for surfaces for which most geometric arrangements have to be inferred indirectly and are always model dependent (Marians and Burdett, 1990). The uneasy feeling prevails that there is a gap in our grasp on the cohesive energy of solids or in the nucleation and growth processes associated with their formation.

Many attempts have been made to systematize charge transfer in solids. Thus, Pauling's second valence rule, in which O atoms function as electron sinks, has in its modern parametric form been applied successfully in systematizing charge transfer between atoms in solids (Brese and

O'Keeffe, 1991; de Jong et al., 2000). Dietzel's cationic field strength and the 15 other different electronegativity scales have been used with varying success in systematizing properties of oxide materials (e.g. Burdett, 1995, 1997). Ketelaar-van Arkel diagrams have been used to assign intuitively the degree of charge transfer in solids (Allen et al., 1993; Jensen, 1995; Mori-Sanchez et al., 2002). Hard-soft acid–base theory and its precursor, Goldschmidt's (1923) atmophile, siderophile, lithophile, and chalcophile classification have rationalized the occurrence of elemental combinations in solids by combining charge transfer with polarizability of the constituent atoms. All these ways of systematizing charge transfer were conceived during the 1920s.

The arrival of computational theoretical chemistry in the 1960s allowed to look with new eyes at charge transfer in solids by examining the atomic orbitals that make up the orthogonal set of molecular orbitals of the system. Isolating characteristic moieties and inspecting the atomic orbital contributions to the overall molecular orbital structure enables testing of the interatomic charge transfer (e.g. Popelier, 2000; Gillespie and Popelier, 2001). It is this atom in a molecule approach, in which one ponders the variation in O atomic orbital coefficients in the molecular orbitals of a molecule, which we shall consider in the following, focusing on O in a surrounding crystalline field. We shall test if, with this notion, at least some part of the gap in our knowledge concerning charge transfer can be bridged.

In some recent studies (Ding et al., 2000, 2005), we looked into the absorbance of atoms and molecules on a ferric oxyhydroxide substrate and attempted to characterize the charge transfer from such substrate to different cations and anions using O1s photoelectron spectroscopy. This spectroscopic technique samples the surficial O layers. Shifts in this O1s spectral line may be correlated with variations of electron density in the valence band as shown in Fig. 30.1. The focus on the O1s core level, with its single or double peak, is advantageous because its spectral interpretation is substantially less complicated and more unequivocal than that of the valence band, which commonly consists of six or more peaks. We concluded from our studies that a solid surface is surrounded by a membrane of O atoms, a two-dimensional O coating on the mineral surface, that varies in charge depending on the nature of the incoming ion. It enabled rationalizations of charge transfer between substrate and adduct in terms of highest occupied (HOMO), which consists primarily of O 2p atomic orbitals, and lowest unoccupied (LUMO) molecular orbitals.

Given the promising nature of these studies we wanted to test if these rationalizations based qualitatively on first principle notions would apply to all oxides and hydroxides for which O1s photoelectron spectra have

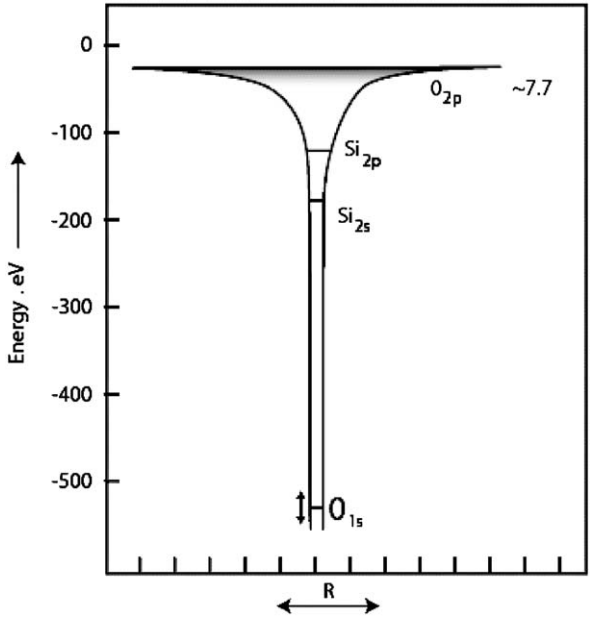

Figure 30.1. The electronic structure of O in silicates. The O1s level varies maximally by about 30 eV according to Bagus and Bauschlicher (1980). The direct gap, i.e. the difference of occupied states on top of the valence band and the continuum is about 7.7 eV for SiO_2 (de Jong, 1989). The top of the valence band consists primarily of O 2p states (de Jong and Brown, 1980).

been recorded; thus that one parameter would suffice to order all acid–base properties of solids and surfaces. We shall show that such parameter does not exist for this close to complete database; that observed surface O charges do not correlate with the standard chemical rationalizations invoking electronegativity variations, and we shall argue that interpretation of surface acid–base properties must include non-bonded electron densities on the O atom. Rather than whole number lone pairs, i.e. two electrons per pair, partially filled lone pairs in Lewis octets coincide with this molecular orbital derived non-bonded electron density concept.

30.2. Method

The overall charge on surface O atom can be ascertained from O1s photoelectron spectroscopy. Bagus and Bauschlicher (1980) calculated the shift in energy of the O1s core level as a function of O valence, i.e. variation in valence electron density, their calculated shifts invalidating

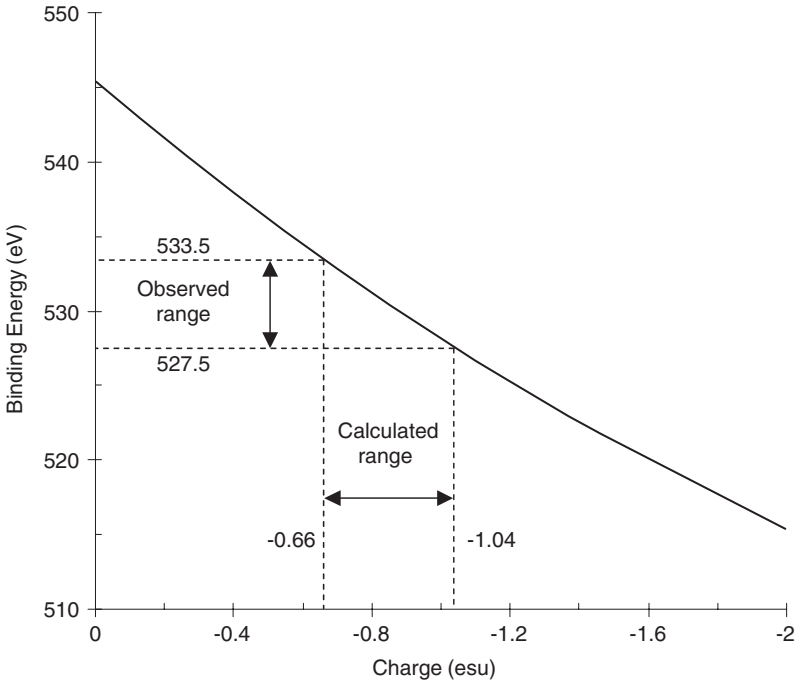

Figure 30.2. O1s core level binding energy versus charge according to Eq. (1) (Ding et al., 2000).

Koopman's theorem which states that the core levels of an atom remain fixed in energy when placed in a compound. Their result is illustrated in Fig. 30.2 and can be couched in the following formula (Ding et al., 2000):

$$Q_{\mathrm{O}} = -4.372 + ((385.023 - 8.976 \times (545.509 - \mathrm{O}_{(1s)}\mathrm{BE}))^{\downarrow}_{\frac{1}{2}})/4.488 \quad (1)$$

where Q_{O} is the valence charge on the O atom in electrostatic units (esu) and $\mathrm{O}_{(1s)}$BE the experimentally determined binding energy in electron Volts (eV).

Some confidence as to the reality of these charges may be inferred from the close correspondence between the one observed for O in SiO_2 and the observed Mulliken charge density for O in state of the art calculations on the $H_6Si_2O_7$ molecule (Burkhard et al., 1991).

We have used this equation to calculate the O charge for the O1s entries of primarily oxides and hydroxides in the NIST XPS database including also some measurements from elsewhere for comparison (de Jong et al., 1994; Barr et al., 1996; Stoecker, 1996). Our results reveal that the variation in O1s core level for oxide materials vary between Cs_2O at

527.5 eV and $Na_2B_4O_7$ at 533.5 eV corresponding to a valence charge difference of 0.38 esu. The absolute values of these core level shifts are not always well determined and especially insulators as SiO_2 show according to the entries in the NIST XPS database a substantial spread in peak position (for SiO_2: 2.3 eV) which may be attributed among others to the well known charging effects of the sample in the absence of a flood gun as for instance pointed out recently by Gijzeman et al. (2003). We have collected the average O charge values for all tabulated inorganic oxides, and hydroxides in Table 30.1. To highlight some of the results, the least negative O charges in this table are the network-forming oxides and hydroxides SiO_2 (−0.698), B_2O_3 (−0.686), $B(OH)_3$ (−0.668), and P_2O_5 (−0.662); the most negative ones Cs_2O (−1.042), PbO_2 (−0.982), PrO_2 (−0.969), Pb_3O_4 (−0.949), and BaO (−0.949).

30.3. Discussion

Previously, we have used O1s surface charges and their variations upon adsorbance of pollutants from aqueous solutions successfully to delineate the charge transfer on ferric oxyhydroxides (Ding et al., 2000, 2005). Here we want to test if this method can be extended to all oxide and hydroxide substrates, and if inter comparison between oxides is possible despite the, in general, lower coordination of surface O atoms relative to bulk ones and the concomitant damped charge difference (El Shafei, 1996).

We shall start this discussion to test if there exists a relation between XPS-derived surface O charge and two bulk solid properties: electronegativity and the difference between solid acids and bases as used in the ceramics and glass industry. Next we shall look if these O surface charges scale with two surface properties of solids: (i) solid acids and bases as proton donors and acceptors respectively, used in heterogeneous catalysis and (ii) points of zero charge variations of solids in contact with aqueous solutions. Finally, we shall discuss the nature of the O charge in terms of bonding and non-bonding electron density by assessing in detail the electronic structure of the valence band of O.

30.3.1. Oxygen charges and electronegativities

The first issue is if the calculated charges can be correlated with observed electron negativity differences between O and the metal atoms in oxides. Of all the available electronegativity scales we did use the one of Allen (1989, 1992) and Murphy et al., (2000) calculated from the valence shell s and p electrons in the ground-state free atoms. This of course leaves out

Table 30.1. O(1s) Binding energy (eV) and calculated O charge Q (esu) for oxides and hydroxides arranged alphabetically

Oxides	$O_{(1s)}$BE (eV)	Q_o (esu)	Oxides	$O_{(1s)}$BE (eV)	Q_o (esu)	Oxides	$O_{(1s)}$BE (eV)	Q_o (esu)
AgO	529.1	−0.936	Fe_3O_4	529.7	−0.898	Pb_3O_4	528.9	−0.949
Ag_2O	529.6	−0.904	FeOOH	530.8	−0.828	PdO	529.4	−0.917
Al_2O_3	531.0	−0.815	$Fe(OH)_3$	531.3	−0.797	PrO_2	528.6	−0.969
As_2O_3	531.9	−0.759	Ga_2O_3	530.9	−0.822	Pr_2O_3	529.2	−0.930
As_2O_5	531.7	−0.772	Gd_2O_3	531.1	−0.809	PtO_2	531.7	−0.772
B_2O_3	533.1	−0.686	GeO_2	532.1	−0.747	$Pt(OH)_2O$	531.1	−0.809
$B(OH)_3$	533.4	−0.668	H_2MoO_4	530.7	−0.834	$Pt(OH)_4$	531.3	−0.797
BaO	528.9	−0.949	H_2WO_4	530.5	−0.847	ReO_2	530.1	−0.872
$Ba(OH)_2$	531.2	−0.803	HfO_2	530.2	−0.866	ReO_3	531.9	−0.759
BeO	531.7	−0.772	HgO	529.9	−0.885	Rh_2O_3	530.6	−0.841
Bi_2O_3	530.0	−0.879	HoO_3	530.6	−0.841	RuO_2	529.4	−0.917
CaO	530.3	−0.859	In_2O_3	530.6	−0.841	RuO_3	530.7	−0.834
$Ca(OH)_2$	531.2	−0.803	$In(OH)_3$	531.8	−0.766	Sb_2O_3	530.0	−0.879
CdO	529.6	−0.904	K(OH)	531.7	−0.772	Sc_2O_3	529.7	−0.898
CdO_2	530.5	−0.847	La_2O_3	530.0	−0.879	SiO_2	532.9	−0.698
$Cd(OH)_2$	531.7	−0.772	Li_2O	531.3	−0.797	Sm_2O_3	530.4	−0.853
CeO_2	529.2	−0.930	Li(OH)	531.2	−0.803	SnO	529.9	−0.885
Ce_2O_3	529.7	−0.898	Lu_2O_3	530.3	−0.859	SnO_2	530.6	−0.841
Ce_3O_4	530.3	−0.859	MgO	530.7	−0.834	SrO	530.4	−0.853
CoO	529.8	−0.891	$Mg(OH)_2$	530.9	−0.822	Ta_2O_5	530.3	−0.859
Co_2O_3	530.1	−0.872	MnO	529.8	−0.891	Tb_2O_3	529.7	−0.898
Co_3O_4	530.0	−0.879	MnO_2	529.6	−0.904	TeO_2	530.4	−0.853
$Co(OH)_2$	531.3	−0.797	Mn_2O_3	529.5	−0.911	ThO_2	530.3	−0.859
CoOOH	530.5	−0.847	Mn_3O_4	529.5	−0.911	TiO_2	530.2	−0.866
CrO_2	529.3	−0.924	Molec. siev	530.5	−0.847	Ti_2O_3	529.6	−0.904
CrO_3	530.1	−0.872	MoO	530.5	−0.847	Tm_2O_3	531.2	−0.803
Cr_2O_3	530.2	−0.866	MoO_2	530.5	−0.847	UO_2	530.3	−0.859

Table 30.1. (*Continued*)

Oxides	$O_{(1s)}$BE (eV)	Q_o (esu)	Oxides	$O_{(1s)}$BE (eV)	Q_o (esu)	Oxides	$O_{(1s)}$BE (eV)	Q_o (esu)
CrOOH	531.2	−0.803	MoO_3	530.6	−0.841	UO_3	530.4	−0.853
$Cr(OH)_3$	531.2	−0.803	Na_2O	529.7	−0.898	U_3O_7	529.9	−0.885
Cs_2O	527.5	−1.042	NaOH	532.8	−0.704	VO_2	530.0	−0.879
Cs_2O_4	530.5	−0.847	Nb_2O_5	530.4	−0.853	V_2O_3	530.4	−0.853
CuO	529.8	−0.891	$Nb_2O_5\cdots OH$	530.7	−0.834	V_2O_4	530.4	−0.853
Cu_2O	530.5	−0.847	Nd_2O_3	530.1	−0.872	V_2O_5	530.2	−0.866
$Cu(OH)_2$	531.1	−0.809	NiO	529.6	−0.904	WO_2	530.7	−0.834
Dy_2O_3	530.6	−0.841	Ni_2O_3	531.6	−0.778	WO_3	530.5	−0.847
Er_2O_3	530.8	−0.828	$Ni(OH)_2$	531.3	−0.797	Y_2O_3	530.0	−0.879
Eu_2O_3	530.8	−0.828	P_2O_5	533.5	−0.662	Yb_2O_3	530.7	−0.834
FeO	530.0	−0.879	PbO	529.4	−0.917	ZnO	530.4	−0.853
Fe_2O_3	529.9	−0.885	PbO_2	528.4	−0.982	ZrO_2	530.7	−0.834

all the transition metal compounds. Inspection of Table 30.1 shows that electronegativity values do not exist on Allen's scale for compounds with an O charge more negative than −0.9 esu. We have collected the remaining variations in electronegativity in Table 30.2 and ordered them in decreasing metal–O ratio.

Inspection of this table shows that the correlation between charge and electronegativity difference is not very strong. For instance in the XO_2 sequence silica, germania, telluria, all metal atoms are four-fold O coordinated, TeO_2 being somewhat exceptional because of its bipyramidal O coordination with four O atoms and one lone-pair located on Te. The O atom in the Te–O bond is expected to be the least negative based on the O–Te electronegativity difference, whereas of the three oxides it has the most negative calculated charge. Electronegativity or parameters that scale with it such as cationic field strength, reflect bulk properties of elements in solids and apparently tend not to scale with surface properties such as the XPS-derived charges.

Table 30.2. Electronegativity differences, Δ, for selected metal–O linkages using Allen's (1989) electronegativity scale in comparison to calculated O valence charge ordered according to metal–O ratio

Compound	Bond	Δ	Charge
X_2O_5			
P_2O_5	O–P	1.36	−0.662
XO_2			
SiO_2	O–Si	1.69	−0.698
GeO_2	O–Ge	1.62	−0.747
TeO_2	O–Te	1.45	−0.853
X_2O_3			
B_2O_3	O–B	1.56	−0.686
Al_2O_3	O–Al	2.00	−0.815
Ga_2O_3	O–Ga	1.85	−0.822
As_2O_3	O–As	1.40	−0.759
In_2O_3	O–In	1.95	−0.841
Sb_2O_3	O–Sb	1.63	−0.879
XO			
BeO	O–Be	2.03	−0.772
MgO	O–Mg	2.32	−0.834
CaO	O–Ca	2.58	−0.859
SrO	O–Sr	2.65	−0.853
SnO	O–Sn	1.79	−0.885
X_2O			
Li_2O	O–Li	2.69	−0.797
Na_2O	O–Na	2.74	−0.898

30.3.2. Oxygen charge and acid–base characteristics of bulk solids

Electronegativity and acidity and basicity are intimately related to one another (e.g. Huheey et al., 1993). For solids two ways exist to distinguish between acids and bases based on the principal species exchanged in acid–base reactions. This is the proton in the Brönsted (1923) theory focusing on its exchange with solid surfaces, and the O atom in the Flood and Forland (1947) and Flood et al. (1947) theory for non-protonic systems, primarily ceramics (e.g. de Jong et al., 1989), for bulk solids. Though our XPS-derived charges tend to reflect only the first three or four O layers of a surface, we tested if these charges scale with the solid acidity parameters for acidic-basic and amphoteric oxides derived by Smith (1987) based on the Flood and Forland (1947) theory. Our results are collected in Table 30.3; Cs_2O with the most negative value, being the most basic oxide; the intermediate negative values being basic or amphoteric oxides,

Table 30.3. Selected values of basic (most negative) and acidity parameters for selected bulk oxides according to Smith (1987) based on the Flood and Forland (1947) concept

Oxide	Parameter acidity	O charge (esu)
Cs_2O	−15.5	−1.042
Na_2O	−12.5	−0.898
BaO	−10.8	−0.949
SrO	−9.4	−0.853
Li_2O	−9.2	−0.797
CaO	−7.5	−0.859
MnO	−4.8	−0.891
MgO	−4.5	−0.834
ThO_2	−3.8	−0.859
CoO	−3.8	−0.891
FeO	−3.4	−0.879
ZnO	−3.2	−0.853
NiO	−2.4	−0.904
BeO	−2.2	−0.772
Al_2O_3	−2.0	−0.815
Fe_2O_3	−1.7	−0.885
Cu_2O	−1.0	−0.847
H_2O	0.0	
ZrO_2	0.1	−0.834
TiO_2	0.7	−0.866
SiO_2	0.9	−0.698
B_2O_3	1.5	−0.686
V_2O_5	3.0	−0.866
WO_3	4.7	−0.847
MoO_3	5.2	−0.841
P_4O_{10}	7.5	−0.662

and the slight negative or positive values being acidic oxides according to Smith (1987). In solution chemistry clearly not all assignments coincide with this classification as inspection of the paper by Rich (1985) concerning the periodicity in acid–base behavior of oxides and hydroxides shows. For example TiO_2 is only soluble in acid and therefore a basic oxide, ZrO_2 and V_2O_5 show a minimum in their solubility as a function of pH and are therefore amphoteric oxides.

Inspection of this table shows that there is no relation between the bulk basicity of a material and the XPS-derived surface charge on the O atom.

30.3.3. Oxygen charge and acid–base properties of oxide surfaces in heterogeneous catalysis

For solid acids and bases used in heterogeneous catalysis acid/base assignments are based on proton exchange between the surface and basic or acidic indicators (Tanabe, 1970) with concomitant color change. This release of protons and associated acid nature of the surface is of significant industrial importance (Izumi et al., 1992; Tanabe and Holderich, 1999). We tabulated those solids collated in Tanabe's book as acid or base and looked at our XPS-derived surface charges including entries besides oxides and hydroxides in the NIST database, and collected the results in Table 30.4.

Inspection of table indicates some global relation between XPS-derived charges and the acidic (proton donor) and basic nature of the surface. Thus, the O charges on the acidic surface tend to be less negative and thus release adsorbed protons easier or accept electron pairs more readily than basic surfaces. Still among acids there are exceptions, MoO_3, TiO_2, V_2O_5, ZnO, and CeO_2, which are according to Tanabe's criterion acids even though they have an O charge more akin to that observed for basic solid oxides.

30.3.4. Acid–base properties of oxide surfaces in aqueous solutions

Finally, a measure of the acid–base character of a surface in aqueous solutions is the point of zero charge. It can be determined either with a zeta potential meter, potentiometric titration or inferred from the minimum in solubility of a compound in aqueous solutions, or the minimum in rate of dissolution (e.g. Kamiya and Shimokata, 1974) as a function of pH. Three solubility behaviors exist: acidic oxides are soluble in base, basic oxides in acids, and amphoteric oxides show a minimum in solubility usually associated with a change in coordination of the dissolved species as for instance observed for alumina (de Jong et al., 1983). Based

Table 30.4. Acid/base characteristics of solid surfaces and the XPS-derived surface charges

Acids	O charge (esu)	Bases	O charge (esu)
$CaCO_3$	−0.797	$BaCO_3$	−0.803
$Al_2(SO4)_3$	−0.729	$CaCO_3$	−0.797
$BaSO_4$	−0.741	Na_2CO_3	−0.772
$CaSO_4$	−0.735	$SrCO_3$	−0.809
$Cr(SO_4)_3$	−0.747	Al_2O_3	−0.815
$CuSO_4$	−0.772	CaO	−0.859
$FeSO_4$	−0.735	Cr_2O_3	−0.866
$Fe_2(SO_4)_3$	−0.759	MgO	−0.834
K_2SO_4	−0.803	SrO	−0.853
$MnSO_4$	−0.729	ZnO	−0.853
$SrSO_4$	−0.747	BaO	−0.949
$ZnSO_4$	−0.723	BeO	−0.770
$AlPO_4$	−0.704	SiO_2	−0.698
$Ca(NO_3)_2$	−0.656		
MoO_3	−0.841		
TiO_2	−0.866		
V_2O_5	−0.866		
CeO_2	−0.930		
ZnO	−0.853		
As_2O_3	−0.759		
SiO_2	−0.698		

on the data of Baes and Mesmer (1976) and Kragten (1978), Rich (1985) has collated a substantial number of these solubility behaviors from which for the amphoteric elements the point of zero charge can be estimated from their minimum in solubility. The scatter in the PZC data is substantial as inspection of the values quoted by Morrison (1985), de Jong (1989), Blesa et al. (1994), Boldyrev (1996), El Shafei (1996), Kosmulski (1997, 2004), and Sposito (2004) show. Some values, such as in particular that for SiO_2 and even Al_2O_3 (Kosmulski, 2003) are open to continuing debate. In Table 30.5, we have collected the pertinent points of zero charge, designated PPZC by Kosmulski (1997), the pristine point of zero charge, versus O charge, the entries coming from the critically assessed canonical set proposed by him. They are arranged in decreasing metal O ratio in accordance with the already by Parks (1965) observed trends in PPZC as a function of this ratio.

Inspection of these PPZC that fulfill tight criteria with respect to their veracity show that they do not correlate with the calculated XPS charges.

Clearly, there seems to be no or only some tentative relation between the various acidity indices and the XPS calculated O charges. Sources of error in the latter may be at the base of this lack of correlation as mentioned previously, because calculating O charges from XPS requires

Table 30.5. O charge and pristine point of zero charge (PPZC) for various oxides (Kosmulski, 1997, 2002a,b)

Compound	PPZC (pH)	O Charge (esu)
X_2O_5		
Nb_2O_5	4.1	−0.853
Ta_2O_5	5.2	−0.859
XO_2		
RuO_2	5.4	−0.917
TiO_2	5.8	−0.866
ZrO_2	7.8	−0.834
CeO_2	8.1	−0.930
HfO_2	7.6	−0.866
X_2O_3		
Fe_2O_3	9.8	−0.885
Al_2O_3	9.1	−0.815
Y_2O_3	9.1	−0.879
Ga_2O_3	9.0	−0.822
In_2O_3	8.7	−0.841
XO		
ZnO	9.2	−0.853
MgO	12.0	−0.834

Table 30.6. Monoxides with the NaCl structure, their density (gr/cc), refractive index, *n*(sodium D line), and XPS-derived surface charge(esu)

Compound	Structure	Symmetry	Density (gr cc–1)	*n*	O charge (esu)
MgO	NaCl	Cubic	3.56	1.737	−0.834
CaO	NaCl	Cubic	3.32	1.837	−0.859
SrO	NaCl	Cubic	4.75	1.870	−0.853
BaO	NaCl	Cubic	5.72	1.980	−0.949
FeO	NaCl	Cubic	5.50	2.320	−0.879
NiO	NaCl	Cubic	6.80	2.270	−0.904

confidence in the absolute value of the O1s energies. However, one may wonder if the overall charge on O is that what determines the interaction of the electron density of this atom with adducting atoms and molecules.

30.3.5. Oxygen charge and the refractive indices of oxides

To assess if something else affects the interaction of O charge density with adducts we have looked at the refractive indices of oxides. As has been well known since Lorentz these refractive indices scale with the number density and dipole oscillator strength of the O atoms in a compound. In Table 3.6, we have collected some oxides with the NaCl structure, their

density, refractive indices (Winchell and Winchell, 1964), and XPS-derived surface charge.

The choice for one structure type presupposes that the surface O atoms in contact with a solvent have a similar O coordination. The XPS-derived O charges are indeed quite similar, even though the bulk refractive indices show large variations, suggesting a very large difference in charge transfer between cation and anion, as may be ascertained from their variation in refractive index, amounting to a maximum variation in light velocity of $43.440\,\mathrm{km\,sec^{-1}}$ between MgO and FeO.

One may wonder why no clear relation exists between variation in overall O charge and any of the material properties of oxides mentioned above. Overall O charge seems not to be the panacea with which to account for a variety of properties, and it may be that the build up of this charge on an O atom in the valence band is what needs to be considered.

30.3.6. Non-bonded electron density on oxygen atoms

The absence of discrete molecules in silicate chemistry in contrast to carbon chemistry was already noted among others by Friedel in the 1870s as one of the principal difficulties in making silicon analogues after carbon-containing molecules. This discreteness of organic molecules made theoretical calculations straightforward in comparison to the extended networks commonly encountered for silicates. It translated in the seventies of the last century in how to calculate an essential silicate moiety embedded in a surrounding, the overall fragment being uncharged. A satisfactory result to account for the spectroscopic properties of silica turned out to be the $H_6Si_2O_7$ molecule (de Jong and Brown, 1980). Isolating the atomic orbitals associated with the Si–O–Si linkage in the overall set of molecular orbitals gave an adequate description of the electronic spectra of quartz, the observed angle bond length variations, as well as charge density on the bridging O atom. Our results indicated that, though the overall O charge remained approximately constant, there was substantial difference in the distribution of this electron density, the top of the valence band containing molecular orbitals that nearly completely consisted of O atomic orbitals only. This charge density was designated the non-bonded O electron density as depicted in Fig. 30.3. It implies that the surface reactivity of oxides hinges on that part of the overall O electron density that is free to react. It is associated with molecular orbitals with the least negative energy, i.e. those orbitals that represent the top of the valence band.

Non-bonded electron density varied as a function of Si–O–Si angle from about four electrons at an Si–O–Si angle of 180 degrees to about 3.5

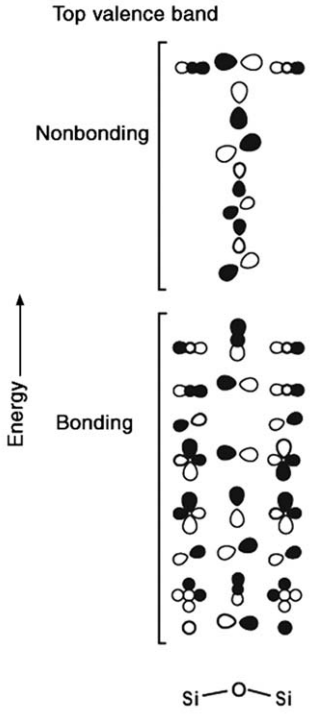

Figure 30.3. Linear combination of atomic orbitals across an Si–O–Si linkage in the $H_6Si_2O_7$ molecule (de Jong, 1989). The overall electron density on the O atom may be partitioned in a bonding and a non-bonding part. Note that the top of the valence band, the highest occupied molecular orbital consists of O 2p states only.

at an angle of 140 degrees, the total number of valence electrons staying about constant around 6.7 electrons, i.e. a valence charge of about –0.7 esu. The four non-bonded electrons on the bridging O correspond to two lone pairs and the rationalization of the virtually always bend Si–O–Si angle in silicates (Liebau, 1985) could readily be rationalized by the Gillespie-Nyholm VSEPR theorem (Gillespie and Popelier, 2001).

Generalizing these results to oxide materials suggests that ionicity or covalency of the constituent bonds in an oxide do not depend on overall charge transfer between O and the atoms in its first coordination sphere. This charge barely varies for surface O as we have demonstrated here. The overall O charge must be partitioned in a part associated with bond formation with atoms in the coordination sphere surrounding the O atoms versus a part on the O atom that is localized on it and free to react and act as an atom in a molecule. It may well be that electronegativity

scales might be used to assess this partitioning into non-bonded and bonded electron density but are likely too crude to account for the variation observed in the complete database. To calibrate this charge transfer additional molecular orbital calculations on different oxide moieties must be carried out to test the variation in O non-bonded electron density for characteristic oxides and hydroxides.

The need for such calculations can be illustrated by examining the electronic structure of two SiO_2 polymorphs: Quartz with ^{IV}Si, each O atom connected to two Si atoms, for which a Lewis octet structure can readily be drawn; and Stishovite with ^{VI}Si, each O atom connected to three Si atoms without an obvious octet structure. The valence band structure for Quartz clearly shows a sizable gap between bonded and non-bonded O 2p states as illustrated in Fig. 30.3. For Stishovite such gap does not exist and the O 2p states are continuous with a total width of 11 eV (Ching, 2000). Thus, despite identical electronegativity differences between the constituent atoms in these two phases, a pronounced variation in O electron density distribution occurs presumably with concomitant surface reactivity, disavowing the possibility of simple rationalizations.

30.4. Conclusion

We have demonstrated previously that it is possible to successfully delineate the HOMO–LUMO interaction between ferric oxyhydroxides and various adsorbing atoms and molecules using XPS-derived O charges and that the HOMO consists primarily of O 2p atomic orbitals. Here, we have attempted to extend our procedure to all oxide and hydroxide materials for which reliable XPS data exist. We have shown that no clear correlation exists between these charges for either bulk properties, i.e. electronegativities, bulk acidity or basicity or refractive indices, or surface properties, solid acids and bases and points of zero charge. Clearly, such generalizations are too primitive and do not represent first principle cause and effect relations. This absence of clear correlations leads us to suggest that rather than considering the overall electron density on the O atom, a distinction has to be made between electrons involved in linking with their surroundings versus those free to react. This image is close to Lewis octet assignments at least for tetrahedrally coordinated oxide materials with their lone versus bond pairs, the difference being that the constraints of complete pairs, i.e. a whole, even number of electrons, must be lifted.

ACKNOWLEDGMENTS

Thoughtful comments by Rebecca Sutton and an anonymous reviewer have aided in improving this manuscript.

REFERENCES

Allen, L.C., 1989. Electronegativity is the average one-electron energy of the valence-shell electrons in ground-state free atoms. J. Am. Chem. Soc. 111, 9003–9014.

Allen, L.C., 1992. Extension and completion of the periodic table. J. Am. Chem. Soc. 114, 1510–1511.

Allen, L.C., Capitani, J.F., Kolks, G.A., Sproul, G.D., 1993. Van Arkel-Ketelaar triangles. J. Mol. Struct. 300, 647–655.

Baes, C.F., Mesmer, R.E., 1976. The Hydrolysis of Cations. Wiley, New York, p. 489.

Bagus, P.S., Bauschlicher, C.W., 1980. Core binding energy shifts for free negative ions of oxygen: O^0 to O^{2-}. J. Electron Spectrosc. 20, 183–190.

Barr, T.L., Seal, S., He, H., Klinowski, J., 1996. X-ray photoelectron spectroscopic studies of kaolonite and montmorillonite. Vacuum 46, 1391–1395.

Blesa, M.A., Morando, P.J., Ragzzonis, A.E., 1994. Chemical Dissolution of Metal Oxides. CRC Press, Boca Raton, p. 401.

Boldyrev, V.V., (Ed.), 1996, Reactivity of Solids: Past, Present and Future. Blackwell Science, Oxford.

Brese, N.E., O'Keeffe, M., 1991. Bond-valence parameters for solids. Acta Crystallogr. B 47, 192–197.

Brönsted, J.N., 1923. Einige bemerkungen über den begriff der Säuren und basen. Recl. Trav. Chim. Pays-Bas 42, 718–728.

Burdett, J.K., 1995. Chemical Bonding in Solids. Oxford University Press, New York, p. 319.

Burdett, J.K., 1997. Chemical Bonds a Dialog. Wiley, Chichester, p. 166.

Burkhard, D.J.M., de Jong, B.H.W.S., Meyer, A.J.M.M., van Lenthe, J.H., 1991. $H_2Si_2O_7$: Ab initio molecular orbital calculations show two geometric conformations. Geochim. Cosmochim. Acta 55, 3453–3456.

Ching, W.Y., 2000. First principles calculation of the electronic structures of crystalline and amorphous forms of SiO_2. In: Devine, R.A.B., Duraud, J.-P., Dooryhee, E. (Eds.), Structure and Imperfections in Amorphous and Crystalline Silicon Dioxide. Wiley, pp. 168–179.

De Jong, B.H.W.S., 1989. Glass, Ullmann's encyclopedia of chemistry and physics. VCH Verlag Weinheim, Ser. A 12, 365–432.

De Jong, B.H.W.S., Adams, J.W., Aitken, B.A., Dickinson, J.E., Fine, G.J., 1989. Glass ceramics, Ullmann's encyclopedia of chemistry and physics. VCH Verlag Weinheim, Ser. A 12, 433–448.

De Jong, B.H.W.S., Brown, G.E., 1980. Polymerization of silicate and aluminate tetrahedra in glasses, melts, and aqueous solutions. I. Electronic structure of H_6Si_2O7, $H_6AlSiO7^{1-}$, and $H_6Al_2O_7^{2-}$. Geochim. Cosmochim. Acta 44, 491–511.

De Jong, B.H.W.S., Ellerbroek, D., Spek, A.T., 1994. Low temperature structure of lithium nesosilicate, Li_4SiO_4, and its Li_{1s} and O_{1s} X-ray photoelectron spectrum. Acta Crystallogr. B 50, 511–518.

De Jong, B.H.W.S., Schramm, C.M., Parziale, V.E., 1983. Polymerization of silicate and aluminate tetrahedra in glasses, melts, and aqueous solutions. IV Aluminum coordination in glasses and aqueous solution and comments on the aluminum avoidance principle. Geochim. Cosmochim. Acta 47, 1223–1236.

De Jong, B.H.W.S., Super, H.T.J., Frijhoff, R.M., Spek, A.L., Nachtegaal, G., 2000. Mixed alkali systems: Dietzel's theorem, X-ray structure, hygroscopicity, and ^{29}Si MASNMR of $NaRbSi_2O_5$ and $NaCaSi_2O_5$. Zeitschrift fuer Kristallographie 215, 397–405.

Ding, M., de Jong, B.H.W.S., Niessen, S.J.B., van der Meer, J.P.M., van Hinsberg, V.J., 2005. Black ferric oxyhydroxide and its sorption of toxic substances. Geochimica 34, 41–50.

Ding, M., de Jong, B.H.W.S., Roosendaal, S.J., Vredenberg, A., 2000. XPS studies on the electronic structure of bonding between solids and solutes: Adsorption of arsenate, chromate, phosphate, Pb^{2+} and Zn^{2+} ions on amorphous black ferric oxyhydroxide. Geochim. Cosmochim. Acta 64, 209–219.

El Shafei, G.M.S., 1996. The polarizing power of metal cations in (hydr)oxides. J. Colloid Interf. Sci. 182, 249–253.

Flood, H., Forland, T., 1947. The acidic and basic properties of oxides. Acta Chem. Scand. 1, 592–604.

Flood, H., Forland, T., Roald, B., 1947. The acidic and basic properties of oxides III relative acid–base strengths of some polyacids. Acta Chem. Scand. 1, 790–798.

Gijzeman, O.L.J., Mens, A.J.M., van Lenthe, J.H., Mortier, W.J., Weckhuysen, B.M., 2003. The effect of chemical composition and structure on XPS binding energies in zeolites. J. Phys. Chem. B 107, 678–684.

Gillespie, R.J., Popelier, P.L.A., 2001. Chemical Bonding and Molecular Geometry. Oxford University Press, New York, p. 268.

Goldschmidt, V.M., 1923. Geochemische Verteilungsgesetze der Elemente. Videnskapsselskapets Skrifter. I. Mat.-naturv. Klasse 3, 3–17.

Huheey, J.E., Keiter, E.A., Keiter, R.L., 1993. Inorganic Chemistry, fourth ed.. HarperCollins, New York, p. 964.

Izumi, Y., Urabe, K., Onaka, M., 1992. Zeolite, Clay, and Heteropoly Acid in Organic Reactions. VCH, Weinheim, p. 166.

Jensen, W.B., 1995. A quantitative van Arkel diagram. J. Chem. Educ. 72, 395–398.

Kamiya, H., Shimokata, A., 1974. The role of salts in the dissolution of powdered quartz. In: Prague Cadek, J., Paces, T. (Eds.), Proc. Int. Symp. Water–Rock Interact.. Czech Geological Survey, pp. 426–429.

Kosmulski, M., 1997. Attempt to determine pristine points of zero charge of Nb_2O_5, Ta_2O_5, and HfO_2. Langmuir 13, 6315–6320.

Kosmulski, M., 2002a. The pH-dependent surface charging and the point of zero charge. J. Colloid Interf. Sci. 253, 77–86.

Kosmulski, M., 2002b. Electric charge density of silica, alumina, and related surfaces. Encyclopedia of Surface and Colloid Science, Ser A, Hubbard ed. Dekker, New York, pp. 1627–1636.

Kosmulski, M., 2003. Point of zero charge of a corundum-water interface probed with optical second harmonic generation and atomic force microscopy: new approaches to oxide surface charge, Comment. Geochim. Cosmochim. Acta 67, 319–320.

Kosmulski, M., 2004. pH dependent surface charging and points of zero charge II Update. J. Colloid Interf. Sci. 275, 214–224.

Kragten, J., 1978. Atlas of Metal–Ligand Equilibria in Aqueous Solution. Ellis Horwood, New York, p. 781.

Liebau, F., 1985. Structural Chemistry of Silicates—Structure, Bonding, and Classification. Springer-Verlag, Heidelberg, p. 347.
Maddox, J., 1988. Crystals from first principles. Nature 335, 201.
Marians, C.S., Burdett, J.K., 1990. Geometric constraints: A refined model for the structure of silica glass. J. Non-Cryst. Solids 124, 1–21.
Mori-Sanchez, P., Martin Pendas, A., Luana, V., 2002. A classification of covalent, ionic, and metallic solids based on the electron density. J. Am. Chem. Soc. 124, 14721–14723.
Morrison, W.H., 1985. Stabilization of aqueous oxide pigment dispersions. J. Coat. Technol. 57, 55–65.
Murphy, L.R., Meek, T.L., Allred, A.L., Allen, L.C., 2000. Evaluation and testing of Pauling's electronegativity scale. J. Phys. Chem. 104, 5867–5871.
Parks, G., 1965. The isoelectric point of solid oxides, solid hydroxides, and aqueous hydroxo complex systems. Chem. Rev. 65, 177–198.
Popelier, P., 2000. Atoms in Molecules: An Introduction. Prentice Hall, New Jersey, p. 164.
Rich, R.L., 1985. Periodicity in the acid–base behavior of oxides and hydroxides. J. Chem. Educ. 62, 44–46.
Smith, D.W.J., 1987. An acidity scale for binary oxides. J. Chem. Educ. 64, 480–481.
Sposito, G., 2004. The Surface Chemistry of Natural Particles. Oxford University Press, New York, p. 242.
Stoecker, M., 1996. X-ray photoelectron spectroscopy on zeolites and related materials. Microporous Mater. 6, 235–257.
Tanabe, K., 1970. Solid Acids and Bases. Academic Press, New York, p. 175.
Tanabe, K., Holderich, W.F., 1999. Industrial application of solid acid–base catalysis. Appl. Catal. A-Gen. 181, 399–434.
Winchell, A.N., Winchell, H., 1964. The microscopical characters of artificial inorganic solid substances: Optical properties of artificial minerals. Academic Press, New York, p. 439.